Journal of Visualized Experiments

Modeling the effects of hemodynamic stress on circulating tumor cells using a syringe and needle

--Manuscript Draft--

Article Type:	Invited Methods Collection - JoVE Produced Video
Manuscript Number:	JoVE62478R1
Full Title:	Modeling the effects of hemodynamic stress on circulating tumor cells using a syringe and needle
Corresponding Author:	Michael Henry University of Iowa Iowa City, IA UNITED STATES
Corresponding Author's Institution:	University of Iowa
Corresponding Author E-Mail:	michael-henry@uiowa.edu
Order of Authors:	Michael Henry
	Devon Moose
	Sophia Williams-Perez
	Renee Cafun
	Benjamin Krog
Additional Information:	
Question	**Response**
Please indicate whether this article will be Standard Access or Open Access.	Standard Access (US$2,400)
Please specify the section of the submitted manuscript.	Cancer Research
Please indicate the **city, state/province, and country** where this article will be **filmed**. Please do not use abbreviations.	Iowa City, IA, USA
Please confirm that you have read and agree to the terms and conditions of the author license agreement that applies below:	I agree to the Author License Agreement
Please provide any comments to the journal here.	
Please indicate whether this article will be Standard Access or Open Access.	Standard Access ($1400)

TITLE:

Modeling the Effects of Hemodynamic Stress on Circulating Tumor Cells Using a Syringe and Needle

AUTHORS AND AFFILIATIONS:

Devon L. Moose[1,2], Sophia Williams-Perez[3], Renee Cafun[1], Benjamin L. Krog[1], Michael D. Henry[1,2,4,5,6]

[1]Department of Molecular Physiology and Biophysics, Carver College of Medicine, University of Iowa, Iowa City, IA 52242, USA
[2]Holden Comprehensive Cancer Center, University of Iowa, Iowa City, IA 52242, USA
[3]MD program, Carver College of Medicine, University of Iowa, Iowa City, IA 52242, USA
[4]Department of Pathology, Carver College of Medicine, University of Iowa, Iowa City, IA 52242, USA
[5]Department of Urology, Carver College of Medicine, University of Iowa, Iowa City, IA 52242, USA
[6]Department of Radiation Oncology, Carver College of Medicine, University of Iowa, Iowa City, IA 52242, USA

SUMMARY:

Here we demonstrate a method to apply fluid shear stress to cancer cells in suspension to model the effects of hemodynamic stress on circulating tumor cells.

ABSTRACT:

During metastasis, cancer cells from solid tissues, including epithelia, gain access to the lymphatic and hematogenous circulation where they are exposed to mechanical stress due to hemodynamic flow. One of these stresses that circulating tumor cells (CTCs) experience is fluid shear stress (FSS). While cancer cells may experience low levels of FSS within the tumor due to interstitial flow, CTCs are exposed, without extracellular matrix attachment, to much greater levels of FSS. Physiologically, FSS ranges over 3–4 orders of magnitude, with low levels present in lymphatics (<1 dyne/cm^2) and the highest levels present briefly as cells pass through the heart and around heart valves (>500 dynes/cm^2). There are a few *in vitro* models designed to model different ranges of physiological shear stress over various time frames. This paper describes a model to investigate the consequences of brief (millisecond) pulses of high-level FSS on cancer cell biology using a simple syringe and needle system.

INTRODUCTION:

Metastasis, or the spread of cancer beyond the initial tumor site, is a major factor underlying cancer mortality[1]. During metastasis, cancer cells utilize the circulatory system as a highway to disseminate to distant sites throughout the body[2,3]. While *en route* to these sites, circulating tumor cells (CTCs) exist within a dynamic fluid microenvironment unlike that of their original primary tumor[3-5]. It has been proposed that this fluid microenvironment is one of many barriers to metastasis[4]. There is wide agreement in the concept of metastatic inefficiency, i.e., that most CTCs entering the circulation either perish or do not form productive metastatic colonies[6-8]. However, why metastasis is inefficient from the perspective of an individual CTC is less certain

and remains an active area of investigation. CTCs are detached from extracellular matrix, deprived of soluble growth and survival factors that may be present in the primary tumor, and exposed to the immune system and hemodynamic forces in a much different manner than in the primary tumor[4]. Each of these factors may contribute to the poor survival of CTCs, but their relative contributions are unclear. This paper addresses the question of how hemodynamic forces affect CTCs.

Studying the effects of hemodynamic forces on CTCs is quite challenging. Currently, there are no engineered *in vitro* systems that can replicate the entire spatiotemporal dynamics (heart to capillaries) and rheological properties of the human vascular system. Moreover, how CTCs experience the circulatory system is not entirely clear. Experimental evidence indicates that most cancer cells do not circulate continuously like blood cells. Rather, due to their relatively large size (10–20 μm in diameter), most CTCs become entrapped in capillary beds (6–8 μm in diameter) for variable lengths of time (s to days) where they may die, extravasate, or be displaced to the next capillary bed[8-11]. However, there is some evidence that CTC size may be more heterogeneous *in vivo,* and that smaller CTCs are detectable[12]. Therefore, based on distance and blood flow velocity, CTCs may only circulate freely for a matter of seconds between these periods of entrapment, although a quantitative description of this behavior is lacking[13].

Furthermore, depending on where CTCs enter the circulation, they may pass through multiple capillary beds in the lung and other peripheral sites and through both the right and left heart prior to reaching their final destination. Along the way, CTCs are exposed to various hemodynamic stresses including fluid shear stress (FSS), compressive forces during their entrapment in the microcirculation, and potentially, traction forces under circumstances where they might exhibit leukocyte-like rolling along blood vessel walls[14]. Thus, both the ability to model the circulation and the understanding of the CTC behavior to be modeled is limited. Because of this uncertainty, any findings from *in vitro* model systems should be validated in an experimental vertebrate organism and ultimately, in cancer patients.

With the aforementioned caveats, this paper demonstrates a relatively simple model to apply FSS to cells in suspension to probe the effects of FSS on CTCs first described in 2012[15]. FSS results from friction of blood flow against the vessel wall, which produces a parabolic velocity gradient under conditions of laminar flow in larger vessels. Cells experience higher levels of FSS near vessel walls and lower levels near the center of the blood vessel. Fluid viscosity, flow rate, and dimensions of the conduit through which the flow occurs influence FSS, as described by the Hagen-Poiseuille equation. This applies to blood flows behaving as Newtonian fluids, but does not hold for the microcirculation. Physiological FSS ranges over several orders of magnitude with the lowest levels in the lymphatics (<1 dyn/cm^2) and the highest at regions around heart valves and atherosclerotic plaques (>500 dyn/cm^2)[5]. Mean wall shear stress in arteries is 10–70 dyn/cm^2 and 1–6 dyn/cm^2 in veins[16,17].

In the heart, cells may be exposed to turbulent flows around valve leaflets where very high-level, but very short-duration FSS may be experienced[18,19]. Although the bioprocessing field has long studied the effects of FSS on mammalian cells in suspension, this information may be of limited

value for understanding the effects of FSS on CTCs as it generally focuses on much lower levels of FSS applied over a long duration[20]. As described below, using a syringe and needle, one can apply relatively high (tens to thousands dyn/cm^2) FSS for a relatively short (milliseconds) duration to a cell suspension. Since the initial description of this model[15], others have employed it to study the effects of FSS on cancer cells[21-23]. Multiple "pulses" of FSS can be applied to cell suspensions in a short period of time to facilitate downstream experimental analyses. For example, this model can be used to measure the ability of cells to resist mechanical destruction by FSS by measuring cell viability as a function of the number of pulses applied. Alternatively, the effects of FSS exposure on the biology of cancer cells can be explored by collecting cells for a variety of downstream analyses. Importantly, part of the cell suspension is reserved as a static control to compare the effects of FSS from those that might be associated with cell detachment and time held in suspension.

PROTOCOL:

1. Cell preparation

1.1. Release cells from tissue culture dish when 70–90% confluent by following the recommended guidelines for the cell line in use.

1.1.1. For example, aspirate the growth medium for PC-3 cells, and wash the 10 cm dish of cells with 5 mL of calcium- and magnesium-free phosphate-buffered saline (PBS).

1.1.2. Aspirate the PBS before adding 1 mL of 0.25% trypsin using manufacturer's protocol.

1.1.3. After observing the detachment of the cells under an inverted microscope, add 5 mL of DMEM:F12 medium containing 10% fetal bovine serum to inhibit the trypsin.

1.2. Place the cell suspension into a conical tube.

1.3. Determine the cell concentration and total cell number.

1.4. Pellet cells by centrifugation (300 × *g* for 3 min), aspirate the supernatant, and resuspend cells in serum-free tissue culture medium to 5 × 10^5 cells/mL.

NOTE: It is critical that the assay medium contains at least 1.17 mM Ca^{++} as extracellular Ca^{++} has been demonstrated to be required for cellular resistance to FSS[15].

2. Fluid shear stress exposure

2.1. Prior to exposing cells to FSS, cut a round-bottom 14 mL polystyrene tube at the 7 mL line. Mix the cell suspension, place 5 mL of the suspension into the cut tube, and collect static control samples.

NOTE: The volume needed to collect for the static sample depends on the viability assay used (see step 3).

2.2. Draw the cell suspension into a 5 mL syringe, and attach a 30 G ½" needle. Uncap the needle, place the syringe onto a syringe pump, secure the syringe, and set the flow rate to achieve the desired level of FSS.

NOTE: **Table 1** shows the maximum wall shear stress for different needles and flow rates, as well as the minimum level of FSS depending on cell size (10, 15, and 20 µm). Inspect the needle prior to use to ensure that it is not bent; if uncertain, replace the needle with a new one. Needle integrity can have significant impact on the level of FSS applied.

2.3. Run the syringe pump, and collect the sheared sample in the cut tube at an approximate 45° angle to reduce foaming. Collect a sample depending on the type of viability assay or downstream assay needs.

2.3.1. Carefully remove the syringe and needle from the syringe pump, and use pliers to remove the needle from the syringe, taking care to not touch the needle.

NOTE: Non-beveled needles can be used interchangeably with beveled needles as an additional safety measure.

2.4. Draw the sheared suspension back into the syringe, carefully reattach the needle using pliers, and place it back into the syringe pump.

2.5. Repeat steps 2.3 and 2.4 until the cell suspension has been exposed to the desired number of pulses of FSS.

NOTE: To assess the capacity of cells to resist mechanical destruction from FSS exposure the cell suspension is typically subjected to 10 pulses of FSS. However, it has been demonstrated that cells start to undergo biological adaptations in response to FSS after 2 pulses[24].

3. Viability measurement

NOTE: Viability can be assessed using enzymatic assays (luciferase, resazurin, and WST-1), counting intact cells, flow cytometry, or by clonogenic assays.

3.1. For all measures of viability, collect a sample prior to exposing cells to FSS.

3.1.1. For enzymatic assays, take duplicate 100 µL aliquots and place them into a 96-well plate.

3.1.2. For flow cytometry, take one 500 µL aliquot and place it into a 1.5 mL tube.

3.1.3. For clonogenic assay, collect a 100 µL aliquot.

3.2. Enzymatic assay

3.2.1. Collect 100 µL samples after 1, 2, 4, 6, 8, and 10 pulses of FSS exposure and place them in a 96-well plate.

3.2.2. Add the desired substrate, and follow the protocol for the assay used:

3.2.2.1. For resazurin, add 20 µL of a 0.15 mg/mL solution to each well. Add 20 µL of 0.15 mg/mL resazurin solution to wells containing 100 µL of medium alone. Incubate for 2 h in a 37 °C tissue culture incubator. Measure the absorbance using a plate reader capable of reading fluorescence (579 excitation/ 584 emission).

3.2.2.2. For luciferase-expressing cells, add 100 µL of 15 mg/mL D-luciferin to 5 mL of medium. Add 100 µL of that solution to each well containing cells. Wait for 5 min, and then read the plate using a reader compatible with luminescence.

3.2.2.3. For WST-1, add 10 µL of WST-1 to each well, including wells containing medium only. Incubate for 4 h, and then read the absorbance between 420 and 480 nm using a plate reader.

3.2.3. Compare the averaged signal from each of the FSS-exposed samples to the averaged static control sample to obtain the percentage of viable cells.

3.3. Flow cytometry[24]

3.3.1. Collect 500 µL samples and place them into 1.5 mL centrifuge tubes after 1, 2, 5, and 10 pulses of FSS.

3.3.2. Centrifuge samples (500 × *g* for 3 min), and discard the supernatants.

3.3.3. Resuspend the pellets with 1 mL of calcium- and magnesium-free PBS, and centrifuge the samples (300 × *g* for 3 min).

3.3.4. Suspend the pellets with 500 µL of fluorescence-activated cell sorting (FACS) buffer (PBS with 0.5% bovine serum albumin and 0.1% sodium azide) with counting beads and membrane-impermeable or viability dyes such as propidium iodide (1.75 µg/mL).

3.3.5. Determine the viability by comparing the ratio of viable cells, normalized to counting beads, in sheared samples to that of the static sample.

3.4. Clonogenic assay

3.4.1. Take 100 µL of the static sample, and add 900 µL of growth medium to make a 1:10 dilution.

3.4.2. Take 100 µL of the 1:10 diluted sample, and add 900 µL of growth medium to make a final 1:100 dilution.

3.4.3. Add 100 µL of the 1:100 dilution sample into each of 3 wells of a 6-well dish containing 2 mL of growth medium.

3.4.4. Repeat steps 3.4.1–3.4.3 with samples that have been subjected to 10 pulses of FSS.

3.4.5. Let the cells grow for 7–10 days without changing the medium, and check for colony formation. Once colonies of ≥50 cells have formed, aspirate the growth medium, rinse each well with 1 mL of PBS, aspirate the PBS, and fix for 5 min using 1 mL of ice-cold 70% ethanol (EtOH). Importantly, fix both sheared and static samples at the same time

3.4.6. After fixing the samples, aspirate the EtOH, and add 1 to 2 mL of crystal violet solution (0.1% crystal violet in 90% H_2O, 10% EtOH) for 5 min.

3.4.7. Rinse with an excess of water, and let the plate dry

3.4.8. Count the colonies (clusters of ≥50 cells) for both the static and sheared samples. Compare the ratio of the average number of colonies from the sheared sample to the average number of colonies from the static sample to determine viability.

REPRESENTATIVE RESULTS:

Elevated resistance to FSS-induced mechanical destruction has been previously shown to be a conserved phenotype across multiple cancer cell lines and cancer cells freshly isolated from tumors relative to non-transformed epithelial cell comparators[15,24]. Here, additional cancer cell lines from a variety of tissue origins (**Table 2**) were tested to demonstrate that the majority of these cells display viability ≥ 20% after 10 pulses of FSS at 250 µL/s. The one exception is MiaPaCa2 cells, which were relatively sensitive to mechanical destruction from FSS (viability ≤ 10%). To adequately describe the FSS resistance profile of a cell line, n ≥ 3 biological replicates are recommended.

By way of comparison, all of the non-transformed epithelial cells examined have viability < 10% under these conditions[15,24]. Thus, while there is a range in FSS resistance observed, the majority of the cancer cell lines tested exhibit greater FSS resistance than non-transformed cells. Cancer cell lines can be derived from both primary tumor tissues and metastases. One could postulate that cells derived from metastases may exhibit greater FSS resistance as this phenotype may have been selected during metastatic dissemination. However, the FSS resistance level was shown to not depend on whether cells were derived from primary tumors or metastases[15,24]. Moreover,

the levels of FSS resistance did not correlate with metastatic potential in a series of human prostate cancer cell lines[15].

To test this further, BALB/c mammary epithelial cells with varying metastatic potential (4T1 = highly metastatic, 4T07 = weak to moderate metastatic potential, 67NR = no to low metastatic potential[25,26]) were used. This experiment revealed that FSS resistance is not correlated with metastatic potential (**Figure 1**). Moreover, both 4T1 and 4T07 cells exhibit a biphasic loss of cell viability—a greater loss of viability in pulses 1–2 than observed in subsequent pulses. This is typical of most cancer cell lines investigated by this group. In contrast, 67NR exhibits a more linear loss of cell viability as a function of FSS. Collectively, the data from **Table 2** and **Figure 1** demonstrate that FSS resistance is a property of transformed cells.

FIGURE AND TABLE LEGENDS:

Figure 1: Fluid shear stress resistance of syngeneic BALB/c mammary epithelial cancer cells. Cells were exposed to FSS (30 G needle, 10 pulses@250 mL/s), and viability was measured using resazurin conversion (n = 4/cell line). While FSS exposure reduced the number of viable cells ($p < 0.0001$, 2-way ANOVA), and each cell line displayed different resistance profiles ($p = 0.0446$, 2-way ANOVA), there was no significant difference among cell lines after 10 pulses of FSS exposure ($p = 0.2833$, 2-way ANOVA). Abbreviations: FSS = fluid shear stress; ANOVA = analysis of variance.

Table 1: Maximum shear stress (τ_{wall}) levels. The table lists the maximum wall FSS levels in dyn/cm^2 for 30 G, 27 G, and 25 G needles at the flow rates of 20, 50, 100, 150, 200, and 250 µL/s. Shear stress levels were calculated using the Poiseuille equation ($\tau_{wall} = {}^{4\mu Q}/_{\pi r^3}$), available information for the inner diameter of each needle gauge, as well as the assumption that µ = 0.01 dyn·s/cm^2. Minimum FSS levels for each size were calculated using $\tau = \tau_{wall}\left(\frac{r}{R}\right)$, wherein r is the radius of cell, and R is the radius of the needle. Abbreviation: FSS = fluid shear stress; τ = shear; τ_{wall} = maximum shear; µ = viscosity; Q = volumetric flow rate.

T**able 2: Fluid shear stress resistance of various cancer cell lines.** Each cancer cell line was exposed to fluid shear stress from the syringe and needle model (30 G needle, 10 pulses@250 mL/s) (n ≥ 3/cell line), and viability was measured either by luciferase activity or resazurin conversion.

DISCUSSION:

This paper demonstrates the application of FSS to cancer cells in suspension using a syringe and needle. Using this model, cancer cells have been shown to be more resistant to brief pulses of high-level FSS relative to non-transformed epithelial cells[15,22,24]. Furthermore, exposure to FSS using this model results in a rapid increase in cell stiffness, activation of RhoA, and increased cortical F-actin and myosin II-based contractility[24,27]. Rapid mechano-adaptation (the ability of CTCs to become more or less stiff depending on the circumstances) may prevent the mechanical destruction of CTCs and facilitate other aspects of metastatic colonization[24,28]. Indeed, findings made using this *in vitro* model have been confirmed using experimental CTCs in animal models[24].

This rapid mechano-adaptation likely explains the bi-phasic loss of cell viability typically observed in this model (**Figure 1**), i.e., FSS-naïve cells are more susceptible to destruction than cells that have been exposed to even a single pulse of FSS. Taken together, this indicates that FSS induces rapid cell stiffening in cancer cells that protects them from subsequent pulses of FSS.

Although the RhoA-actomyosin axis is an important driver of FSS resistance[15,21,24], there are likely other mechanisms involved[29]. Further evidence that cell stiffness is a key determinant of FSS resistance is that disruption of lamin A, which controls the structural integrity of the nucleus—the stiffest component of the cell, reduces FSS resistance in cancer cells using this model[22]. We are using this model to probe the mechanisms of FSS resistance in cancer cells further. Here, this model has been used to measure the capacity of various cancer cell lines to resist mechanical destruction by exposing cells to brief pulses of high levels of FSS. Although this is a relatively inexpensive, simple model to develop in the laboratory, with the most expensive element being the syringe pump, care must be taken to follow the protocol faithfully to obtain reproducible results. Multiple pulses of FSS can be applied to cells in a very short time, <10min. The total elapsed time for the experiment depends on the suspension volume, flow rate, pulse number, and the dexterity of the user transferring the suspension between pulses. With experience, a 5 mL suspension exposed to FSS with a 30 G needle for 10 pulses@250 µL/s can be processed in ~10 min. For most cell lines, there is minimal loss of viability due to being held in suspension for this length of time.

Because the exposure to FSS occurs relatively quickly, FSS is typically applied to cell suspensions in serum-free medium to reduce foaming of the samples. The difference in viscosity between 0–10% fetal bovine serum is negligible in this assay. However, it is critical to ensure physiologic levels of calcium in the medium in which the cells are sheared. Moreover, with regard to the methods for cell dissociation prior to FSS exposure, no difference in FSS resistance was detected in PC-3 cell suspensions prepared by trypsinization or treatment with non-enzymatic dissociation agents[15]. Cell concentration can be greater or less than 5×10^5 cells/mL depending on downstream application needs. The response of PC-3 prostate cancer cells is similar in a range from 5×10^4 to 5×10^5[,15]. However, the effects of cell concentration on viability after FSS exposure should be empirically determined.

For most applications envisioned with cultured cells, cell density should not significantly affect viscosity and therefore, the amount of FSS applied. Variables, such as the time for which the cells are held in suspension prior to FSS exposure, should be held constant across experimental replicates. As mentioned above, needle integrity is also critical. Lot variations have been noted in needles with respect to this assay over time. Hypodermic needles were designed for clinical use, not for the flow rates employed here. On rare occasions, the hub of the needle can be partially occluded, which during subsequent pulses, occludes the passage of suspension through the needle and ultimately, backflow around the syringe plunger. Further, it is very important to understand that dead/dying cells are exceptionally sensitive to FSS, as shown previously[24]. Therefore, if a particular cell line has a high level of dying cells, either as a routine characteristic or experimental manipulations (e.g., drug treatments), this will result in a very steep loss of cell viability that might not be completely normalized by comparison to the static control.

The application of FSS can be paired with other assays, such as immunofluorescence, pulldown assays, and western blotting, to study the effect of FSS on cancer cell biology [24]. In principle, this model might also be used to explore the effects of high-level, short-duration FSS on other cell types including blood cells. Normal red blood cells and leukocytes are much more resistant to FSS applied in this way than even cancer cells, which stands to reason physiologically[15]. In fact, the level of FSS applied, using a 30 G ½" needle at a flow rate of 250 mL/s, brackets the range required for the disruption of the red cell membrane (based on millisecond application of force)[30,31]. One limitation of this model, or any that involve passing fluid through a conduit, is that the precise level of FSS that cells experience within the range from the maximum wall shear stress and the minimum at the center of the conduit is not known. Thus, at each pulse, all the cells do not experience the same level of FSS, and over repeated pulses, individual cells would be expected to experience different levels of FSS at each pulse within the range specified.

However, hydrodynamic focusing under the conditions employed in this model results in cells being directed toward the center of the flow, away from the wall, and thus toward lower FSS exposure[32]. Other models, such as cone and plate viscometers or Couette chambers, are better suited for the application of FSS at constant levels to a cell suspension. As mentioned above, it remains challenging to model FSS exposure of CTCs *in vitro*. This model is best suited to test the effects of high, but brief, exposure to FSS as might happen traversing the heart. Flow through arteries and veins results in longer exposure to lower levels of FSS. However, as mentioned, how long CTCs remain in continuous flow in the circulation is unclear, and most experimental evidence to date is consistent with short periods (seconds) of free flow punctuated by longer periods of entrapment in the microcirculation.

Models that expose cancer cells in suspension to lower levels of FSS (0.5–60 dyn/cm^2) for longer durations (minutes to days) include cone and plate viscometers, Couette chambers, continuous flow loops, syringe with a tube extension, and microfluidic devices[33-37]. These have also been used to gain insights into how FSS might affect CTCs and have led to finding that exposure to FSS increases oxidative stress, cell proliferation and invasion, and stem cell-like characteristics in various cancer cell lines. It will be interesting to compare results derived from those models with the one described here. For example, using a continuous flow loop model, Xin et al. found that the ROCK-actomyosin axis promoted a *loss of cell viability* in cancer cell lines exposed to FSS (20 dyn/cm^2) for 2–12h in stark contrast to the data described above[38]. Thus, biological context is very likely to matter for all of these *in vitro* models, reinforcing the need to translate findings about CTCs into *in vivo* models and ultimately, cancer patients.

ACKNOWLEDGMENTS:

Development of the model demonstrated here was supported by DOD grant W81XWH-12-1-0163 and NIH grants R21 CA179981 and R21 CA196202.

DISCLOSURES:

MDH is a co-founder, President and shareholder of SynderBio, Inc. DLM is a consultant for SynderBio, Inc.

REFERENCES:

1 Dillekås, H., Rogers, M. S., Straume, O. Are 90% of deaths from cancer caused by metastases? *Cancer medicine.* **8** (12), 5574–5576 (2019).

2 Hanahan, D., Weinberg, R. A. Hallmarks of cancer: the next generation. *Cell.* **144** (5), 646–674 (2011).

3 Strilic, B., Offermanns, S. Intravascular survival and extravasation of tumor cells. *Cancer Cell.* **32** (3) 282–293 (2017).

4 Labelle, M., Hynes, R. O. The initial hours of metastasis: the importance of cooperative host-tumor cell interactions during hematogenous dissemination. *Cancer Discovery.* **2** (12), 1091–1099 (2012).

5 Krog, B. L., Henry, M. D. Biomechanics of the circulating tumor cell microenvironment. *Advances in Experimental Medicine and Biology.* **1092**, 209–233 (2018).

6 Weiss, L. Metastatic inefficiency. *Advances in Cancer Research.* **54**, 159–211 (1990).

7 Zeidman, I., Mc, C. M., Coman, D. R. Factors affecting the number of tumor metastases; experiments with a transplantable mouse tumor. *Cancer Research.* **10** (6), 357–359 (1950).

8 Fidler, I. J. Metastasis: quantitative analysis of distribution and fate of tumor embolilabeled with 125 I-5-iodo-2'-deoxyuridine. *Journal of the National Cancer Institute.* **45** (4), 773–782 (1970).

9 Cameron, M. D. et al. Temporal progression of metastasis in lung: cell survival, dormancy, and location dependence of metastatic inefficiency. *Cancer Research.* **60** (9), 2541–2546 (2000).

10 Luzzi, K. J. et al. Multistep nature of metastatic inefficiency: dormancy of solitary cells after successful extravasation and limited survival of early micrometastases. *American Journal of Pathology.* **153** (3), 865–873 (1998).

11 Kienast, Y. et al. Real-time imaging reveals the single steps of brain metastasis formation. *Nature Medicine.* **16** (1), 116–122 (2010).

12 Takagi, H. et al. Analysis of the circulating tumor cell capture ability of a slit filter-based method in comparison to a selection-free method in multiple cancer types. *International journal of molecular sciences.* **21** (23), 9031 (2020).

13 Scott, J., Kuhn, P., Anderson, A. R. Unifying metastasis--integrating intravasation, circulation and end-organ colonization. *Nature Reviews Cancer.* **12** (7), 445–446 (2012).

14 Wirtz, D., Konstantopoulos, K., Searson, P. C. The physics of cancer: the role of physical interactions and mechanical forces in metastasis. *Nature Reviews Cancer.* **11** (7), 512–522 (2011).

15 Barnes, J. M., Nauseef, J. T., Henry, M. D. Resistance to fluid shear stress is a conserved biophysical property of malignant cells. *PLoS One.* **7** (12), e50973 (2012).

16 Malek, A. M., Alper, S. L., Izumo, S. Hemodynamic shear stress and its role in atherosclerosis. *JAMA.* **282** (21), 2035–2042 (1999).

17 Brass, L. F., Diamond, S. L. Transport physics and biorheology in the setting of hemostasis and thrombosis. *Journal of Thrombosis and Haemostasis.* **14** (5), 906–917 (2016).

18 Stein, P. D., Sabbah, H. N. Turbulent blood flow in the ascending aorta of humans with normal and diseased aortic valves. *Circulation Research.* **39** (1), 58–65 (1976).

19 Strony, J., Beaudoin, A., Brands, D., Adelman, B. Analysis of shear stress and hemodynamic factors in a model of coronary artery stenosis and thrombosis. *The American Journal of Physiology.* **265** (5 Pt 2), H1787–1796 (1993).

20 Chalmers, J. J. Mixing, aeration and cell damage, 30+ years later: what we learned, how it affected the cell culture industry and what we would like to know more about. *Current Opinion in Chemical Engineering.* **10**, 94–102 (2015).
21 Vennin, C. et al. Trsient tissue priming via ROCK inhibition uncouples pancreatic cancer progression, sensitivity to chemotherapy, and metastasis. *Science Translational Medicine.* **9** (384),126 (2017).
22 Mitchell, M. J. et al. Lamin A/C deficiency reduces circulating tumor cell resistance to fluid shear stress. *American Journal of Physiology: Cell Physiology.* **309** (11), C736–746 (2015).
23 Ortiz-Otero, N. et al. Cancer associated fibroblasts confer shear resistance to circulating tumor cells during prostate cancer metastatic progression. *Oncotarget.* **11** (12), 1037–1050 (2020).
24 Moose, D. L. et al. Cancer cells resist mechanical destruction in circulation via RhoA/actomyosin-dependent mechano-adaptation. *Cell Reports.* **30** (11), 3864–3874 (2020).
25 Miller, B. E., Miller, F. R., Wilburn, D. J., Heppner, G. H. Analysis of tumour cell composition in tumours composed of paired mixtures of mammary tumour cell lines. *British Journal of Cancer.* **56** (5), 561–569 (1987).
26 Aslakson, C. J., Miller, F. R. Selective events in the metastatic process defined by analysis of the sequential dissemination of subpopulations of a mouse mammary tumor. *Cancer Research.* **52** (6), 1399 (1992).
27 Chivukula, V. K., Krog, B. L., Nauseef, J. T., Henry, M. D., Vigmostad, S. C. Alterations in cancer cell mechanical properties after fluid shear stress exposure: a micropipette aspiration study. *Cell Health Cytoskeleton.* **7**, 25-35 (2015).
28 Gensbittel, V. et al. Mechanical adaptability of tumor cells in metastasis. *Developmental Cell.* **56** (2), 164–179 (2021).
29 O'Leary, B. R. et al. Pharmacological ascorbate inhibits pancreatic cancer metastases via a peroxide-mediated mechanism. *Scientific Reports.* **10** (1), 17649–17649 (2020).
30 Williams, A. R., Hughes, D. E., Nyborg, W. L. Hemolysis near a transversely oscillating wire. *Science.* **169** (3948), 871–873 (1970).
31 Rooney, J. A. Hemolysis near an ultrasonically pulsating gas bubble. *Science.* **169** (3948), 869–871 (1970).
32 Connolly, S., McGourty, K., Newport, D. The in vitro inertial positions and viability of cells in suspension under different in vivo flow conditions. *Scientific Reports.* **10** (1), 1711–1711 (2020).
33 Brooks, D. E. The biorheology of tumor cells. *Biorheology.* **21** (1–2), 85–91 (1984).
34 Triantafillu, U. L., Park, S., Klaassen, N. L., Raddatz, A. D., Kim, Y. Fluid shear stress induces cancer stem cell-like phenotype in MCF7 breast cancer cell line without inducing epithelial to mesenchymal transition. *Internation Journal of Oncology.* **50** (3), 993–1001 (2017).
35 Fan, R. et al. Circulatory shear flow alters the viability and proliferation of circulating colon cancer cells. *Scientific Reports.* **6**, 27073 (2016).
36 Fu, A. et al. High expression of MnSOD promotes survival of circulating breast cancer cells and increases their resistance to doxorubicin. *Oncotarget.* **7** (31), 50239–50257 (2016).
37 Li, S. et al. Shear stress promotes anoikis resistance of cancer cells via caveolin-1-dependent extrinsic and intrinsic apoptotic pathways. *Journal of Cellular Physiology.* **234** (4), 3730–3743 (2019).

482 38 Xin, Y. et al. Mechanics and actomyosin-dependent survival/chemoresistance of
483 suspended tumor cells in shear flow. *Biophysical Journal.* **116** (10), 1803–1814 (2019).
484

Figure

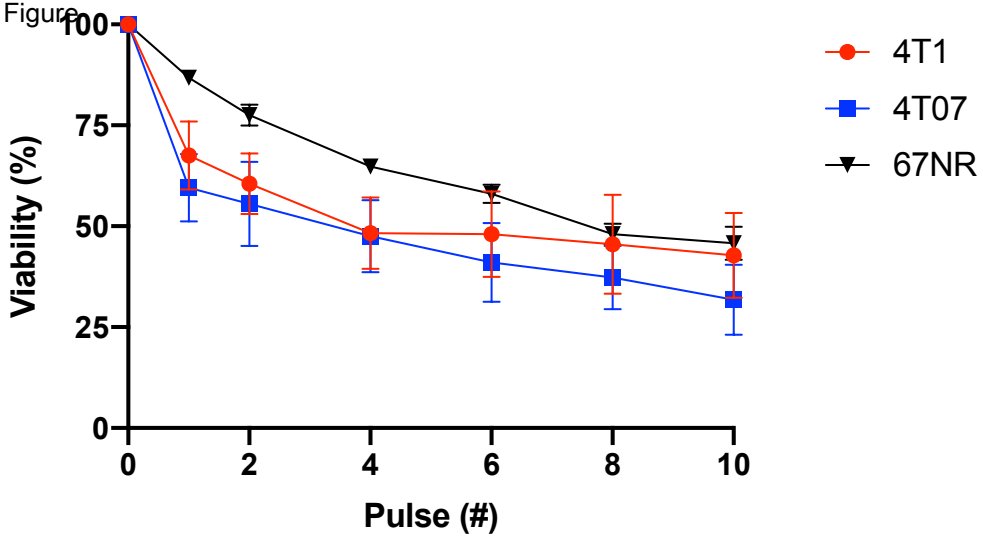

Table 1

Shear (τ):		wall (maximum)					
Cell Diameter:		N/A			10 µm		
Needle Gauge:		30	27	25	30	27	25
Flow Rate (µL/s)	20	507	220	116	32	10	4
	50	1267	550	290	80	26	11
	100	2534	1100	580	159	52	22
	150	3801	1650	869	239	79	33
	200	5068	2200	1159	319	105	45
	250	6335	2750	1449	398	131	56

	minimum				
	15 µm			20 µm	
30	**27**	**25**	**30**	**27**	**25**
48	16	7	64	21	9
120	39	17	159	52	22
239	79	33	319	105	45
359	118	50	478	157	67
478	157	67	637	210	89
598	196	84	797	262	111

Table 2

Cell Line	Tissue Source	Species	Mean Viability (%) after 10 pulses
TRAMPC1	Prostate	Mouse	40
4T01	Breast	Mouse	32
4T7	Breast	Mouse	43
67NR	Breast	Mouse	46
66CL4	Breast	Mouse	28
RT4	Bladder	Human	62
W17-266-4	Melanoma	Human	46
HS852	Melanoma	Human	41
HS695	Melanoma	Human	41
A2058	Melanoma	Human	37
A375	Melanoma	Human	37
RPMI-7951	Melanoma	Human	35
SKMEL2	Melanoma	Human	29
A101D	Melanoma	Human	28
MiaPaCa	Pancreatic	Human	7

Name of Material/ Equipment	Company	Catalog Number	Comments/Description
0.25% Trypsin	Gibco	25200-056	
14 mL round bottom tubes	Falcon - Corning	352059	
30 G 1/2" Needle	BD	305106	
5 mL syringe	BD	309646	
96-well black bottom plate	Costar - Corning	3915	
Bioluminescence detector	AMI	AMI HTX	
BSA, Fraction V	Sigma	10735086001	
Cell Titer Blue	Promega	G8081	
crystal violet	Sigma	C0775	
D-luciferin	GoldBio	D-LUCK	
DMEM	Gibco	11965-092	
FBS	Atlanta Biologicals	S11150	
PBS	Gibco	10010023	
Plate Reader	BioTek	Synergy HT	
Sodium Azide (NaN_3)	Sigma	S2002	
Syringe Pump	Harvard Apparatus	70-3005	

Roy J. and Lucille A. Carver College of Medicine
University of Iowa

Michael D. Henry, Ph.D.
The Department of
Molecular Physiology & Biophysics
6-510 Bowen Science Building
Iowa City, Iowa 52242-1109
319-335-7886 ***Tel***
319-335-7330 ***Fax***
michael-henry@uiowa.edu

1 April, 2021

Amit Krishnan, Ph.D.
Review Editor
JoVE
amit.krishnan@jove.com
617.674.1888

Re: Rebuttal Letter for JoVE62478 "Modeling the effects of hemodynamic stress on circulating tumor cells using a syringe and needle"

Dear Dr. Krishnan,

We thank the reviewers for their comments. Below we respond to their *concerns* in red.

Reviewer #1
Major Concerns:
1) The protocol is literally injecting cells through a syringe and needle. It seems self-explanatory based on the authors' original paper, and I would ask what the added advantage of publishing this very simple protocol might be to readers and anyone with any reasonable skill in cell culture. Perhaps the authors can clearly lay out in their intorduction why this protocol is needed over and above published papers. For example, I see that the authors have included a table to calculate FSS based on needle diameter and flow rate. While this can be calculated based on the authors previous work; perhaps having it in a protocol would make it more convenient / adoptable. Please outline the challenges that new users might face when trying this out, and therefore motivate the need for this protocol to be available.

We appreciate the reviewer's point. Although this is a relatively straightforward protocol, we do get questions from time to time about implementing this model, reproducibility, etc. where a video would be helpful. We have added additional information on calculating maximum and minimum levels of FSS exposure (see below). Challenges are outlined in the Discussion as directed by the Instructions to Authors.

2) From a theoretical fluid mechanics point of view, it seems like cells in the laminar flow region of the needle would experience different FSS depending on their radial position within the needle. The authors acknowledge this in the context of in vitro larger vessels; but they do not acknowledge it as a limitation / source of error in their experimental system. The inner diameter of a 30G needle is 160 microns, which is 16x bigger than average diameter of a circulating cells. Hence, I would strongly recommend that this error be characterized and reported, as FSS

can range from ZERO at the channel center to the max value at the wall, resulting in highly heterogenous stimulation profiles. This heterogeneity is also likely the cause for repeated pulses causing increased loss of viability with pulse cycles - the gradual reduction in viability may be due to some cells being sheared while others are not each cycle.

Yes, the cells are exposed to a range of FSS in the conduit and we do note this as a limitation in paragraph 3 of the Discussion: "*One limitation of our model, or any that involve passing fluid through a conduit, is that the precise level of FSS that cells experience within the range from the maximum wall shear stress and the minimum at the center of the conduit is not known."* We also refer readers to other models where uniform levels of FSS can be applied and cite other relevant work in the field on inertial focusing in our type of model which will tend to drive cells toward the center of the flow, away from the walls. We further address the reviewer's comment by expanding Table 1 to include minimum levels of FSS at the axis of flow which is a function of cell diameter. We have included several cell diameters in this table and report the formula for calculating this for any cell diameter. As cells are not dimensionless, FSS at the axis of flow never reaches zero. Thus, at each pulse all of the cells do not experience the same level of FSS, and over repeated pulses, individual cells would be expected to experience different levels of FSS at each pulse within the range specified. We have added this sentence to paragraph #3 of the discussion for clarity.

Reviewer #2

Major Concerns:

There is a significant body of literature on the effect of hydrodynamic forces on cells, many focused on bioprocessing. Several studies have attempted to summarize those studies and it would be very valuable for the current manuscript to not only mention this, but put there cell data in context (compare) to those other studies. Further, there are a number of studies in last 10 years looking at the effect of potential pumps to pump human blood. Obviously, fluid forces are important in those devices, and the current would should also be put in the context of those studies.

Some of those studies:

A cost-effective and reliable method to predict mechanical stress in single-use and standard pumps; Ina Dittler, Stephan C. Kaiser1, Katharina Blaschczok, Christian Löffelholz, Pascal Bösch, Wolfgang Dornfeld, Reto Schöb, Jürgen Rojahn, Matthias Kraume, Dieter Eibl; Eng. Life Sci. 2014, 14, 311-317

Mixing, aeration and cell damage, 30+ years later: what we learned, how it affected the cell culture industry and what we would like to know more about; Jeffrey J Chalmers; Current Opinion in Chemical Engineering 2015, 10:94-102

We understand the Reviewer's comment but, respectfully, find it difficult to integrate this additional large field of important literature into this much narrower description of our method here. The objective of much of the work in the bioreactor field is to understand and minimize the effects of fluid shear stress on

cellular damage to optimize production. Generally speaking, bioreactors work at much lower levels of FSS for much longer durations (hours-weeks) than does our model. Additionally there much more literature that one could review on the effects of fluid shear stress on cells (and how to model it) that we see as outside the scope of this methods paper and instead have tried to focus on models specifically aimed at mimicking the effects of fluid shear stress on circulating tumor cells. However, in deference to the reviewer's comment we have added the following sentence citing the reference above: "Although the bioprocessing field has long studied the effects of FSS on mammalian cells in suspension, this information may be of limited value for understanding the effects of FSS on CTCs as it generally focuses on much lower levels of FSS applied over a long duration."

Minor Concerns:
There is significant literature data that shows that not all CTC are as large as 10-15 microns claimed in the manuscript.

Yes, we acknowledge this and have provided a supporting reference. The size of CTCs is heterogeneous and some smaller CTCs are detected.

What enzyme viability assay was used??

This is a Cell Titer Blue (Resazurin) assay, which is now specified.

Reviewer #3
Major Concerns: None.

Minor Concerns: None.

Sincerely,

Michael Henry
Professor
Depts. of Molecular Physiology and Biophysics and Pathology and Urology and Radiation Oncology
Deputy Director for Research, Holden Comprehensive Cancer Canter
The University of Iowa
Iowa City, IA 52242